

Foxa1 and Foxa2 Control Bile Duct Development

Zhaoyu Li, Peter White, Geetu Tuteja, Nir Rubins, Sara Sackett and Klaus H.

Kaestner*

Department of Genetics and Institute of Diabetes, Obesity and Metabolism,
School of Medicine, University of Pennsylvania, Philadelphia, PA 19104, USA

* correspondence to: kaestner@mail.med.upenn.edu

752B CRB

415 Curie Blvd.

Philadelphia, PA 19104-6145

Phone: 215-898-8759

Fax: 215-573-5892

Supplemental Materials

Methods

Staining for β -Galactosidase Activity

To identify the fidelity of Cre expression in the AlfpCre transgenic lines, the founders were crossed to the Rosa26 reporter line (1) and embryos collected at embryonic day 10.5. Briefly, the embryos were dissected and fixed for 1 h in 4%PFA at 4°C. After washing with PBS, the embryos were embedded in OCT. X-Gal staining were applied to the whole embryos and sagittal cryostat sections.

Primer Sets for Quantitative PCR (qPCR)

Gene	Forward	Reverse
Foxa1	CAAGGATGCCTCTCCACACTT	TGACCATGATGGCTCTCTGAA
Foxa2	GAGCACCATTACGCCTTCAAC	AGGCCTTGAGGTCCATTTTGT
Alb	TCAGGTGTCAACCCCAACTCT	TCCACACAAGGCAGTCTCTGA
Ttr	GGTTTTCACAGCCAACGACTC	GGATGCTACTGCTTTGGCAAG
Afp	CCTCCCAGTGCGTGACGGAGAA	CACTTCCTCCTCGGTGGCTTCC
Jag-1	AACACAGGGATTGCCCACTT	TGTTGCAATCAGGACCCATC
Hes1	AGAGGCTGCCAAGGTTTTTG	TCCCACTGTTGCTGGTGTAGA
Tgfb1	GTTTAATTGACCCCGAGGAGC	GAGAAGAGAGCGCAGAATCCA
Tgfb1r	GGACCTAATGCTGGCCTGAC	TGAGCGAGGTTAGGGTGGTT
Egf	TGCCTCAGAAGGAGTGGGTTA	GTGTTCCAAGCGTTCCTGAGA
Wnt7b	TCCCCTGTCTGTCATGTCTCTT	CTGTTTCAAGCAGAAGGAGGAG
Hnf6	CAAATCACCATCTCCCAGCAG	CAGACTCCTCCTCCTGGCATT

Hnf1b	CATCTGCAATGGTGGTCACAG	GGCTTGCAGTGGACACTGTTT
Hnf4a	ATGACACGTCCCCATCTGAAG	CTCGAGGCTCCGTAGTGTTTG
Nfkb(p50)	TGAACTCCGGGATAGTGACAG	GTGGGCTGTCTCCAGTAAGAGA
GR	AGGCGATACCAGGATTCAGA	GCAAAGCATAGCAGGTTTCC
Gp80	AAGCAGCAGGCAATGTTACC	CATAAATAGTCCCCAGTGTCG
Gp130	AGGGGAAGAATATGCTGTGC	AAGTGCCATGCTTTGACTGG
CK19	ACTTGCGCGACAAGATTC	AACTTGGTTCTGAAGTCATCTGC
CK7	ACAAATTCGCCTCCTTCATC	TTGGCTGACTTCTGTTCTG
CK20	GCACAGATTAAAGAGCTGCAA	GTCCTCTGCAGCCAGCTTAG
Ki67		
Fgl1	GTTCTCTCAGTGGGAAGAATGG	TCTGCACAAGAGGCTTACCC

Primer Sets for Chromatin Immunoprecipitation (ChIP)

Genomic locus	Strand	Primers
Foxa1/2_IL6_prom1	Forward	TTACCCACCTGGCAACTCCT
	Reverse	TGCTTGTTTTTCTGTGTCTTG
Foxa1/2_IL6_prom2	Forward	TCTGCTCACTTGCCGGTTT
	Reverse	AAGTAGGGAAGGCCGTGGTT
Foxa1/2_IL6_prom3	Forward	CCTGAACAAAGGAGACCCCTA
	Reverse	CCAAATGCTCTGTATTTACCAAGAAC
GR_IL6_prom1	Forward	CACTGGGGAGAATGCAGAGA
	Reverse	CAGGTGGGTAAAGTGGGTGAA
GR_IL6_prom2	Forward	TGGAAGCCAAGATTGCTTGA

	Reverse	TCCAAATTTTGTGCAGTTGTTTC
Nfkb_IL6_prom	Forward	GACATGCTCAAGTGCTGAGTCAC
	Reverse	AGATTGCACAATGTGACGTCG

References

1. Soriano, P. 1999. Generalized lacZ expression with the ROSA26 Cre reporter strain. *Nat Genet* 21:70-71.

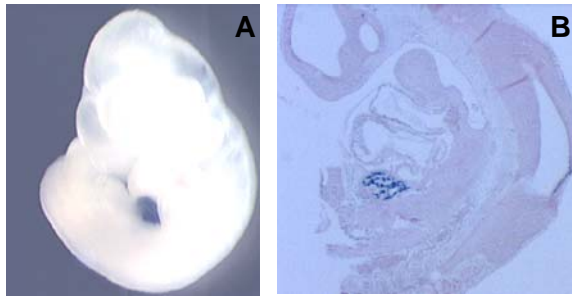


Fig. S1

AlfpCre transgene expresses at embryonic day 10.5 (E10.5). AlfpCre transgenic mice were crossed to the Rosa26 reporter mice (1). X-gal staining of the whole embryos (A) and sagittal sections (B) showed β -galactosidase/Cre activity in the liver primordium at E10.5.

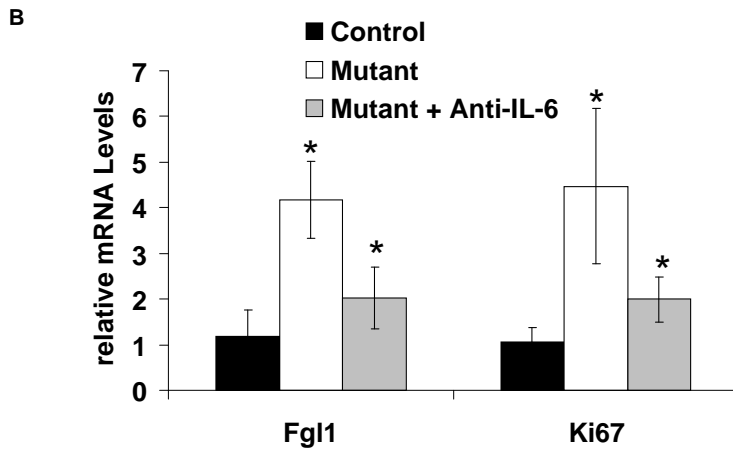
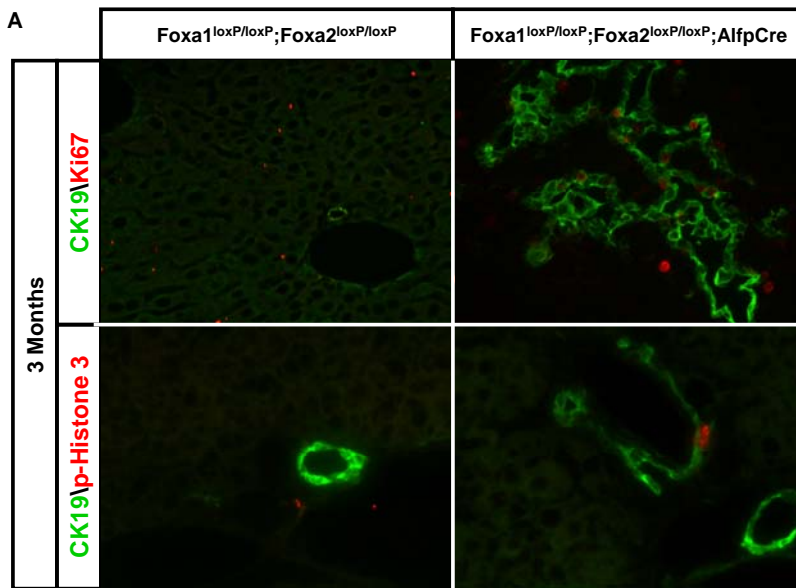


Fig. S2

Foxa1/2 deficiency induces bile duct proliferation. (A) Immunofluorescent staining of OCT-embedded liver sections from 3-month old of Foxa1^{loxP/loxP};Foxa2^{loxP/loxP} (Control) and Foxa1^{loxP/loxP};Foxa2^{loxP/loxP};AlfpCre (Mutant) mice with anti-CK19 (green), anti-Ki67 (red) and anti-phospho-histone 3 (p-Histone 3, red) antibodies. (B) Hepatic mRNA levels of fibrinogen-like 1 (Fgl1) and Ki67 from 3-month old control, mutant mice and mutant mice after the treatment of IL-6 antagonist as determined by quantitative real-time RT-PCR. *, $P < 0.05$ from comparison between mutant and control mice.

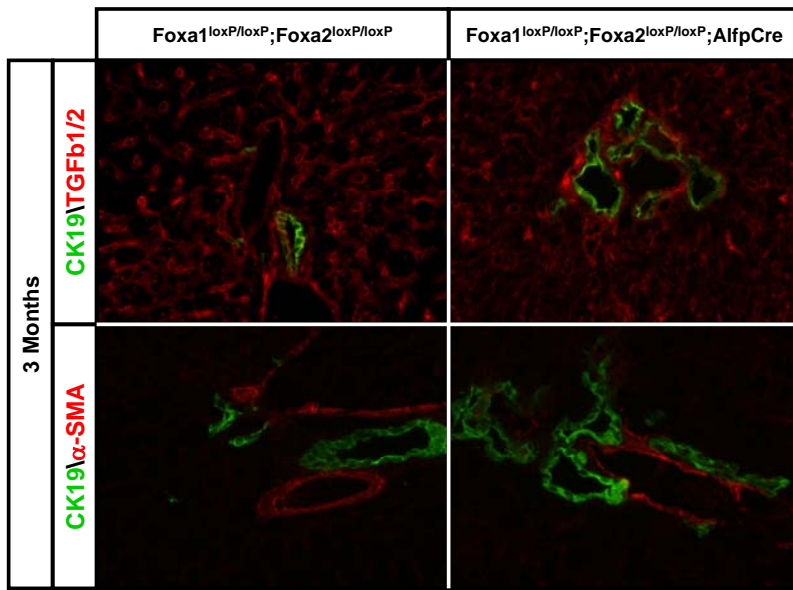


Fig. S3

Immunofluorescent staining of OCT-embedded liver sections from 3-month old of Foxa1^{loxP/loxP};Foxa2^{loxP/loxP} (Control) and Foxa1^{loxP/loxP};Foxa2^{loxP/loxP};AlfpCre (Mutant) mice with anti-CK19 (green), anti-TGFb1/2 (red) and anti-alpha smooth muscle actin (α -SMA, red) antibodies.

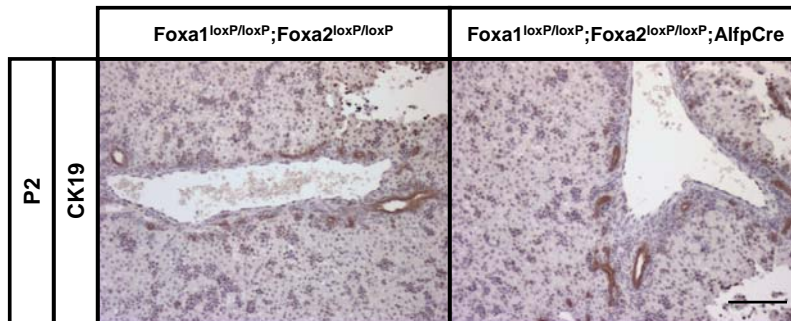


Fig. S4

Foxa1/2 deficiency does not affect the formation of ductal plates. Immunohistochemical staining of paraffin-embedded liver sections from postnatal day 2 (P2) Foxa1^{loxP/loxP};Foxa2^{loxP/loxP} (Control) and Foxa1^{loxP/loxP};Foxa2^{loxP/loxP};AlfpCre (Mutant) mice with an anti-CK19 antibody.

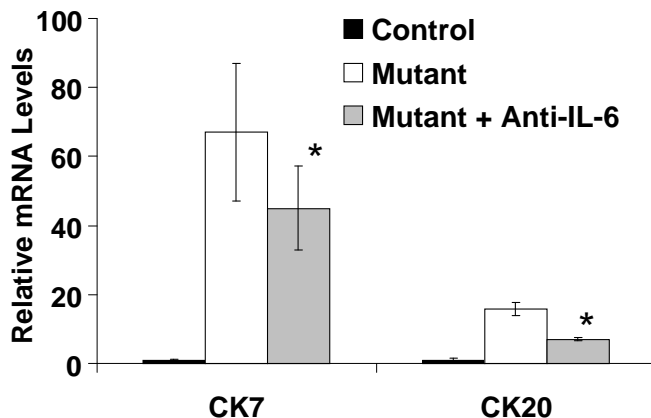


Fig. S5

Hepatic mRNA levels of CK7 and CK20 from embryonic day 14.5 (E14.5), postnatal day 2 (P2) and 3-month old of Foxa1^{loxP/loxP};Foxa2^{loxP/loxP} (Control) and Foxa1^{loxP/loxP};Foxa2^{loxP/loxP};AlfpCre (Mutant) mice and mutant mice after the treatment of anti-IL-6 antibody by quantitative real-time RT-PCR. *, $P < 0.05$ from comparison between mutant and anti-IL-6 antibody treated mutant mice.

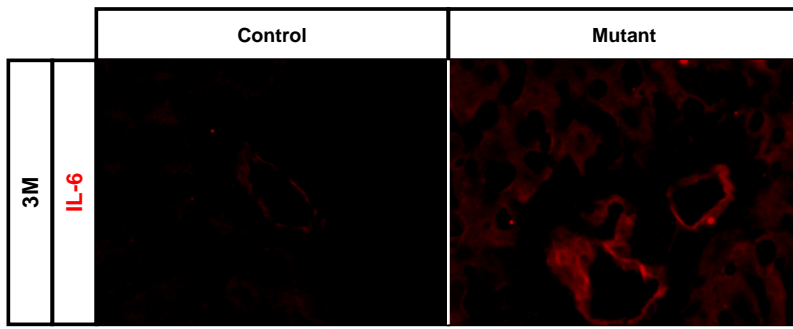


Fig. S6

Immunofluorescent staining of OCT-embedded liver sections from 3-month old of $Foxa1^{loxP/loxP};Foxa2^{loxP/loxP}$ (Control) and $Foxa1^{loxP/loxP};Foxa2^{loxP/loxP};AlfpCre$ (Mutant) mice with anti-IL-6 (red) antibodies.

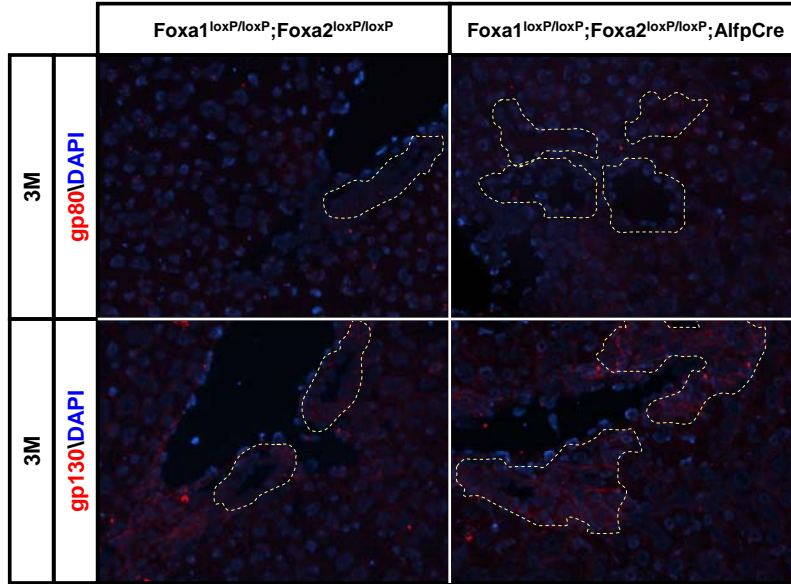


Fig. S7

Immunofluorescent staining of OCT-embedded liver sections from 3-month old of $Foxa1^{loxP/loxP};Foxa2^{loxP/loxP}$ (Control) and $Foxa1^{loxP/loxP};Foxa2^{loxP/loxP};AlfpCre$ (Mutant) mice with DAPI (blue), anti-gp80 (red) and anti-gp130 (red) antibodies. The dot lines enclose bile ducts

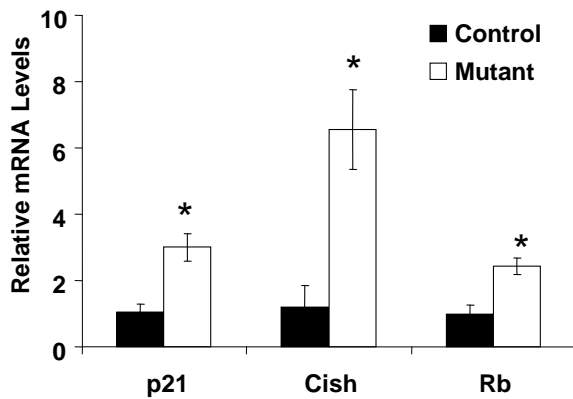


Fig. S8

Hepatic mRNA levels of p21, Cish and Rb from 3-month old of $Foxa1^{loxP/loxP};Foxa2^{loxP/loxP}$ (Control) and $Foxa1^{loxP/loxP};Foxa2^{loxP/loxP};AlfpCre$ (Mutant) mice by quantitative real-time RT-PCR. *, $P < 0.05$ from comparison between mutant and control mice.